Development of an Absolute Quantification Method for hERG Using PRM with Single Isotopologue in-Sample Calibration

Ge Chang, Fabusuyi A. Aroge, Ravichandra Venkateshappa, Tom W. Claydon, and Bingyun Sun*

Read Online

ACCESS | Metrics & More | Article Recommendations

ABSTRACT: The human ether-à-go-go-related gene (KCNH2)-encoded protein hERG constitutes the α subunit of the Kv11.1 channel and contributes to the I_{kr} current, which plays an important role in the cardiac action potential. Genetically and xenobiotically triggered malfunctions of hERG can cause arrhythmia. The expression of hERG in various study systems was assessed mainly as the fold change relative to the corresponding control. Here, we developed a simple and sensitive quantitation method using targeted mass spectrometry, i.e., the parallel reaction monitoring approach, to measure the absolute quantity of hERG in copy number. Such measurements do not require controls, and the obtained values can be compared with similar results for any other protein. To effectively avoid matrix effects, we used the heavy-match-light (HML) in-sample calibration approach that requires only a single isotopologue to achieve copy-number quantitation. No significant difference was observed in the results obtained by HML and by the classic standard addition in-sample calibration approach. Using four proteotypic peptides, we quantified the average number of copies of hERG in the HEK293T heterologous expression system as $3.6 \pm 0.5 \times 10^6$ copies/cell, i.e., 1 million copies/cell for the fully assembled Kv11.1 channel.
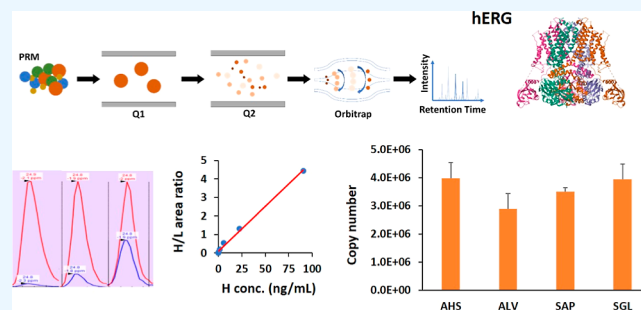
INTRODUCTION

The human ether-a-go-go-related gene (KCNH2) encodes the alpha subunit of a voltage-gated tetrameric potassium ion channel (Kv11.1), which contributes to the rapid delayed rectifier current, I_{kr}, in human cardiomyocytes.[1] I_{kr} functions at the late stage of the cardiac action potential to repolarize the membrane, which is critical for maintaining a normal cardiac contraction rhythm. The protein encoded by human ether-a-go-go-related gene is commonly referred to as hERG.[2,3] Despite its homologous structure with other potassium ion channels, the kinetics of hERG are unique because its activation process is much slower than its inactivation process.[4] Such kinetics render the ion channel to open slowly during the rapid depolarization phase in the cardiac action potential before rapid inactivation occurs. Upon cell plasma membrane repolarization, the channel recovers from its inactivation to the open conformation, resulting in a tail current in the late stage of repolarization of the cardiac membrane potential. This process effectively controls the QT interval in the electrocardiogram of the heart and prevents arrhythmia by preventing "early after-depolarization, EAD".[5,6]

Mutations that trigger gain or loss functions of hERG are a known cause of channelopathy, such as short or long QT syndrome,[5,7,8] respectively. Similar symptoms are also elicited by blockers and activators of the normal channel (i.e., class III antiarrhythmics) as well by off-target effects caused by a wide-variety of other noncardiac drugs including vasodilators, psychiatric drugs, antimicrobial and antimalarial drugs, and antihistaminics, such as Bepridil, Amitryptiline, Clarythromycin, and Astemizole.[9] Life-threatening off-target effects on the Kv11.1 channel have forced the withdrawal of many drugs from the market. Consequently, the test of Kv11.1 blockage is a routine practice in early drug development.

Changes in both the structure and expression of hERG contribute to clinically observed gains and losses of channel functions, which can be caused by genetic mutations, environmental risk factors, aging, and drug toxicity. In addition to channelopathy, clinical malfunction of hERG is also linked to various other medical conditions, such as obstructive sleep apnea, ischemic heart diseases, and pulmonary diseases,[10] in which patients do not carry hERG mutations. Moreover, hERG is often overexpressed in cancer cells, which has been linked to the role of hERG in cell proliferation, tumor invasion, and neoangiogenesis.[11−13] In nonexcitable cells, hERG function is
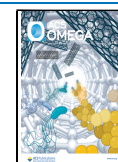
believed to be switched off but is rapidly activated upon entry into the mitotic cycle.[14]

Accurate quantitation of hERG is paramount for biochemical and biomedical studies of the channel. Common approaches for quantifying hERG are transcript-centric and protein-centric methods. RNA-centric analyses such as qRT-PCR[15] and RNA-seq[16] offer high specificity for the hERG transcript; however, they do not directly quantify the hERG protein.[17,18] For protein-centric quantitation, electrophysiology[19−21] can probe channel function such as the I_{kr}, and immunochemical approaches can measure protein quantity; however, antibody-based approaches could lack specificity. For frequently employed qRT-PCR and Western blotting quantification approaches for hERG, the results are relative and need to be normalized to a loading control with stable expression. The use of single protein/gene loading controls is highly debated, as many studies have shown that in the heart, the commonly used loading controls themselves exhibit variable expression.[22−24] ELISA-based immunoassays can provide absolute quantifications if pure protein standards with known concentrations are available. Many successful ELISA assays have been developed for quantifying cytosolic proteins and secreted signaling molecules such as cytokines and chemokines; however, for endogenous ion channel proteins including hERG, direction quantification remains elusive due to the complex structure and membrane localization of the protein.

The alpha subunit of Kv11.1, hERG, possesses six trans-membrane alpha helices: two of which are used to form the ion-conducting pore and the other four are used for voltage sensing.[3] This subunit also hosts two N-glycosylation sites and numerous phosphorylation sites.[3] Expressing and purifying known amounts of hERG as a standard for absolute quantitation via ELISA is challenging. Tagged hERG has been engineered to substitute the native protein for quantitation purposes.[25]

Like transcript-centric analysis, mass spectrometry (MS)-based quantitation provides direct protein-centric analysis that possesses high specificity,[26,27] and the results can be either relative or absolute in quantity[27−30] with no need for loading controls or purified whole proteins as standards. To provide a useful tool for studying hERG, we develop here a MS-based and targeted parallel reaction monitoring (PRM) assay for the absolute quantification of hERG. Our assay takes advantage of the recently published single-isotopologue in-sample calibration approach[31] that uses heavy-match-light (HML) mathematical treatment to quantify the endogenous analyte. We also compared the analysis results with those of the classic standard addition (SA) in-sample calibration approach. Four unique and proteotypic peptides of hERG were selected for assay development, which ensured high specificity. An Orbitrap was employed as the mass analyzer to provide high accuracy and high sensitivity in the PRM assay. We applied the developed assay to quantify the copy number of hERG in the HEK293T heterologous expression system.

■ MATERIALS AND METHODS

Materials. Sequence-grade bovine pancreas TPCK-treated trypsin (EC 3.4.21.4) was obtained from Worthington Biochemical Co. (Lakewood, NJ, USA). Tris(2-carboxyethyl)-phosphine (TCEP), dithiothreitol (DTT), iodoacetamide (IAA), and protease inhibitor cocktail were obtained from Sigma-Aldrich (St. Louis, MO, USA). Trypan blue staining was obtained from Lonza (Walkersville, Maryland, United States). The bicinchoninic acid (BCA) Protein Assay Kit (cat. 23227)

was obtained from Pierce Thermo Fisher (Waltham, MA, USA). An MCX cartridge (cat. 186000252) was obtained from Waters (Milford, MA, USA). Four unique hERG peptides, i.e., ALVGPGSPPR (ALV), SAPGQLPSPR (SAP), AHSLNP-DASGSSCSLAR (AHS), and SGLLNSTSDSDLVR (SGL), with C13- and N15-incorporated arginine, were synthesized by JPT Peptide Technologies (Berlin, Germany). ALV and SGL were also synthesized from regular light isotopes by GenicBio Limited (Shanghai, China). Dulbecco's modified Eagle's medium (DMEM), fetal bovine serum (FBS), and the remaining chemicals were obtained from Fisher Scientific (Pittsburgh, PA, USA). The polyclonal antibody against hERG (cat. PA3−860) and the monoclonal antibody against GAPDH (cat. MA5−15738-D800) were obtained from Invitrogen (Waltham, MA, USA).

Cell Harvest. HEK293T cells transfected with hERG (HEK293T-hERG) were cultured in DMEM supplemented with 10% FBS at 37 °C and 5% CO_2. The cells were transfected with hERG cDNA subcloned into a pCDNA3 vector using Lipofectamine 3000 (Invitrogen) and harvested 44−48 h after transfection in Versene solution (0.2 g EDTA per liter of PBS) for analysis. Trypan blue was used to count the cells with a hemocytometer. Finally, the cell suspension was pelleted by centrifugation (300−500g) and stored at −20 °C for further analysis.

Protein Extraction and Tryptic Digestion. Protein extraction and tryptic digestion were carried out following a previously described protocol[32,33] with slight modifications. In detail, the cell pellet was dissolved in lysis buffer (10 mM EDTA, 10 mM TCEP, 0.3% SDS in 40 mM Tris, pH 8.0). Solvation of the sample was facilitated by heating to 100 °C in a water bath for 10 min and sonicating by a probe sonicator for 10 min with pauses. The protein concentration was measured through a BCA assay.

Prior to proteolysis, the samples were treated with 8 M urea at 37 °C with end-to-end rotation for 30 min to completely denature the proteins. Then, cysteine residues were alkylated by incubating the sample with 15 mM IAA in the dark at room temperature for 30 min, and the reaction was quenched by incubating the sample with 20 mM DTT for 15 min at room temperature. The resolved mixtures were diluted 10-fold with PBS to reduce the SDS and urea concentrations to less than 0.05% and 1 M, respectively, prior to trypsin addition at an enzyme-to-protein ratio of 1:50. The digestion was carried out overnight at 37 °C with end-to-end rotation. The completion of digestion was verified by SDS-PAGE with silver staining before the samples were purified with MCX cartridges. The cleaned peptides were dried in a SpeedVac (model SPD121P-230, Thermo Scientific, Mississauga, ON, Canada) and stored at −20 °C.

LC−MS/MS Analysis. The digested and cleaned samples were reconstituted in MS loading buffer (0.1% formic acid, FA) before LC−MS/MS analysis by an EASY nLC 1000 coupled with a Q Exactive HF Hybrid Quadrupole-Orbitrap Mass Spectrometer through a nano-EASY spray source (Thermo Scientific, Mississauga, ON, Canada). Separation was carried out using commercial Pepmap EASY-spray C18 trap and analytical columns (Thermo Scientific, Mississauga, ON, Canada) with 75 μm ID and 3 μm C18 resin with 100 Å pore size at lengths of 20 and 150 mm, respectively, for a 60 min gradient of 2−35% buffer B (0.1% FA in acetonitrile), as detailed previously.[34] A voltage of 2.0 kV was used for electrospray, and the ion transfer tube that guided ions into the MS was heated to 250 °C.

To discover the proteotypic peptides that were suitable for PRM quantitation, the data-dependent acquisition (DDA) method was used to select the top 10 most abundant precursor ions in the MS1 scan for higher energy collisional dissociation (HCD) fragmentation with a dynamic exclusion of 10 s. The MS1 scans were acquired in the m/z range of 400−2000 with a mass resolution of 120,000, and the MS2 resolution was 30,000. The automatic gain control (AGC) values for the MS1 and MS2 scans were 1×10^6 and 2×10^5, respectively. Precursors with charges of 1+ or >5+ were excluded from MS2 scans, and the default charge was 2+.

For the PRM analysis, two in-sample calibration strategies were used. First was the recently developed HML approach,[31] in which synthetic heavy peptides were spiked in a sample at known concentrations as calibrators, and the corresponding endogenous hERG peptides were used as internal standards to construct calibration curves. Second was the classic SA approach, in which synthetic light peptides from hERG were spiked in the sample at known concentrations as the calibrators, and the corresponding heavy synthetic peptides were also spiked in the sample as the internal standards to construct the calibration curves. In the SA analysis, light synthetic peptides at 7 different concentrations plus buffer-alone condition (from 0 to 0.5 μg/mL) and heavy synthetic peptides at fixed concentrations (0.13 and 0.19 μg/mL for ALV and SGL, respectively) were added to 8 aliquots of cleaned sample peptides derived from HEK293T-hERG lysates at a volume ratio of 1:1:8. In the HML approach, heavy synthetic peptides at 8 concentrations, including the buffer-alone control, were spiked into 8 aliquots of cleaned sample peptides from the same HEK293T-hERG lysate for final concentrations ranging from 0 to a maximum of 0.053−0.093 μg/mL depending on the particular peptide. Three repeated PRM analyses were performed for each sample aliquot.

The Q Exactive HF parameters for PRM analysis were MS1 scan with a m/z range of 400−2000, a mass resolution of 120,000, an AGC target of 3×10^6, and a maximum ion injection time of 200 ms. For the MS2 scans, the parameters were as follows: mass resolution, 30,000; AGC target, 2×10^5; maximum ion injection time, 150 ms; and isolation window, 2.0 Th, with a 0.5 Th offset to include additional isotopic peaks, as previously reported.[31] The MS2 scans were conducted based on the inclusion list that included the m/z ratio of the endogenous light and the corresponding heavy reference peptides of hERG and a duration of more than 10 min scheduled around the elution peaks of every target peptide. To ensure the best fragmentation, the collisional energy was systematically varied from 17 to 35 normalized collision energies (NCE).

To evaluate assay reproducibility, 3 repeated LC−MS/MS analyses were carried out on different days for every dilution set. Furthermore, three independent sample preparations were performed on the same biological sample; two of them were used for HML analysis, and the other was used for SA analysis. In total, we carried out 72 LC−MS/MS runs. For each transition of every selected peptide, 8 concentrations were used to construct the calibration curve.

Data Analysis. The raw files acquired from DDA analyses by Xcalibur (Thermo Fisher Scientific) were searched by Proteome Discoverer 2.1 (Thermo Fisher Scientific, Mississauga, ON, Canada) using Sequest HT. A customized database was used, which combined the human UniProt database and common contaminants. The monoisotopic precursor mass tolerance was 10 ppm, and the monoisotopic fragment mass tolerance was 0.02 Da. The criteria for accessing full tryptic peptides included a

minimum of 6 amino acids and 2 miss cleavages. Cysteine carbamidomethylating (+57.051 Da) was treated as a static modification; methionine oxidation (+15.995 Da), asparagine and glutamine deamidation (+0.984 Da), serine and threonine phosphorylation (+79.966 Da), and protein N-terminal acetylation (+42.011 Da) were treated as dynamic modifications. The reversed sequences of the human UniProt database were used to assess the false discovery rate (FDR). A strict FDR cutoff of 0.01 and Percolator were used to filter the confident identifications.

The analysis of the PRM results was performed using Skyline v21.1.[35] Initially, 11 transitions, including 3 precursor signals (monoisotopic peak M and two additional isotopic peaks, $M + 1$ and $M + 2$) and the top 8 fragment signals from both the endogenous light peptides and heavy peptides, were used for assay development. All signal peak boundaries were manually checked before exporting the chromatographic peak area from Skyline for analysis. A calibration curve was constructed for each transition of every peptide by plotting the signal area ratios between the calibrator and the internal standard as a function of the calibrator concentration. Specifically, for the SA approach, L/H peptide area ratios were plotted against the final concentrations of the light peptides. For the HML method, H/L peptide area ratios were plotted against the concentrations of heavy peptides. Least square linear regression analysis was applied to obtain the calibration curves. Only the curves with the coefficient of determination of no less than 0.96 were used for further evaluation. The lower limit of quantification (LLOQ) was computed as LLOQ = 10 s/m,[36] where s is the standard deviation of the responses in the control conditions ($N = 3$) in the HML method and m is the slope of the calibration curve. The SA method cannot be used to determine the LLOQ owing to the lack of control conditions for assessing the standard deviation.

To calculate the endogenous peptide concentrations, the methods used for SA and HML were different. For HML analysis, the concentration of endogenous peptides was calculated by $\frac{1 - \text{intercept}}{\text{slope}}$ as described in a previous publication.[31] For SA analysis, the concentration was obtained by $\frac{\text{intercept}}{\text{slope}}$. The copy number of the corresponding hERG inferred from individual peptides in the cell was obtained by converting the peptide concentration to the number of peptide molecules and averaging it across the total number of cells used for analysis.

A two-tailed Dixon's Q test[37,38] was carried out on the computed concentrations of the endogenous light peptides, and results with Q values above the 99% confidence level of the Q table were removed as outliers. A two-tailed t-test in Microsoft Excel was used to analyze the quantitation difference in results obtained by HML and SA methods, and $p < 0.05$ was the cutoff for statistical significance. One-way ANOVA was used to analyze the variations among copy numbers obtained from four targeted peptides, and $p < 0.05$ was considered for statistical significance.

Western Blot. Lysates from HEK293T-hERG cells and control HEK-293T cells were resolved by SDS-PAGE and subsequently transferred to the PVDF membrane. Primary antibodies recognizing hERG and the loading control, GAPDH, were incubated with the membranes at 4 °C overnight, separately, and then visualized by the WesternBreeze antirabbit Chromogenic Kit (cat. WB7105, Invitrogen).

Table 1. Peptides Confidently Detected in hERG by the DDA Approach[a]

Confidence	Annotated Sequence[a]	PSMs[b]	Position in hERG
High	GHVAPQNTFLDTIIR	5	6-20
High	AEVMQRPcTcDFLHGPR	3	57-73
High	GPPTSWLAPGR	6	149-159
High	LKLPALLALTAR	4	165-176
High	SGGAGGAGAPGAVVVDVDLTPAAPSSESLALDEVTAMDNHVAGLGPAEER	4	182-231
High	SGGAGGAGAPGAVVVDVDLTPAAPSSESLALDEVTAMDNHVAGLGPAEERR	3	182-232
High	ALVGPGSPPR	5	233-242
High	SAPGQLPSPR	8	243-252
High	AHSLNPDASGSScSLAR	6	253-269
High	EScASVR	4	274-280
High	ASSADDIEAmR	3	282-292
High	AGVLPPPPR	8	293-301
High	SGLLNSTSDSDLVR	5	313-326
High	IPQITLNFVDLKGDPFLASPTSDR	4	333-356
High	IPQITLNFVDLKGDPFLASPTSDREIIAPK	3	333-362
High	VTQVLSLGADVLPEYK	6	374-389
High	DTNMIPGSPGSTELEGGFSR	3	864-883
High	RTDKDTEQPGEVSALGPGR	4	894-912
High	TDKDTEQPGEVSALGPGR	5	895-912
High	SSDTcNPLSGAFSGVSNIFSFWGDSR	8	980-1005
High	QYQELPR	4	1008-1014
High	cPAPTPSLLNIPLSSPGR	3	1015-1032
High	LSADMATVLQLLQR	11	1056-1069
High	LSLPGQLGALTSQPLHR	3	1136-1152
Phosphopeptides			
High	ALVGPGsPPR	3	233-242
High	RLsLPGQLGALTSQPLHR	3	1135-1152
High	IPQITLNFVDLKGDPFLASPTSDREIIAPK (unidentified phosphosites)	4	333-362

[a]Red highlights the peptides selected for PRM quantitation, and green highlights the peptides used to evaluate digestion efficiency. [b]Modified amino acids are in small captions. [c]PSM stands for peptide spectrum match.
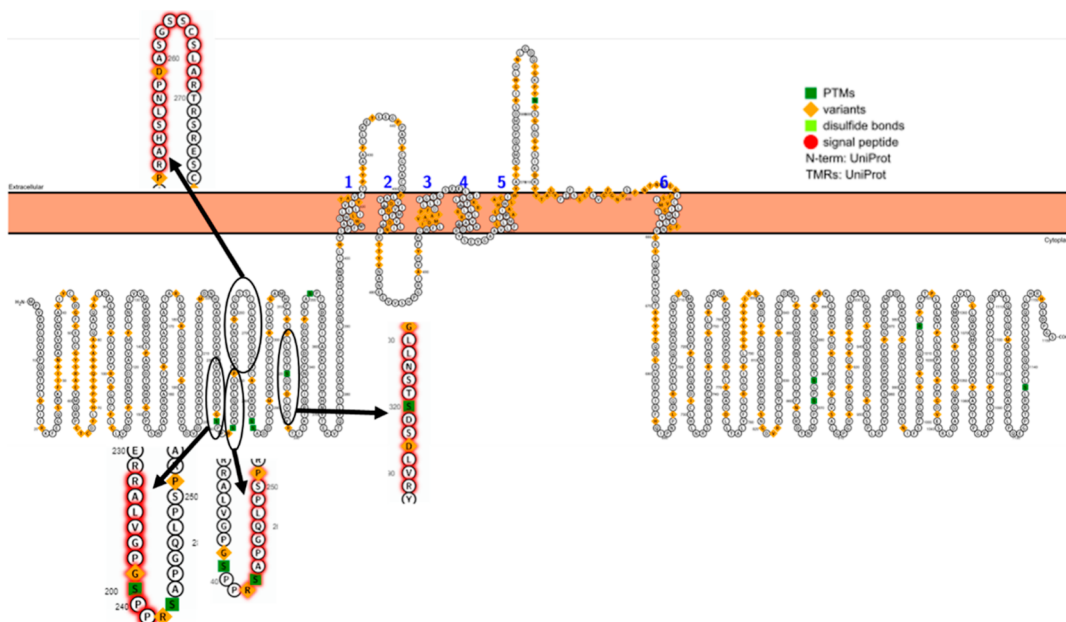

Figure 1. Illustration by Protter[40] of the hERG membrane topology and the selected surrogate peptides.

■ RESULTS AND DISCUSSION

Selection of Surrogate Peptides and Their Corresponding Transitions for hERG Quantitation. For a successful PRM assay, suitable target peptides are critical. These peptides need to be specific to the target proteins and carry high ionization and proteolysis efficiency, together with many other desired properties, such as being free of modifications.[26,39] Several amino acids are prone to modifications, including S, T, and Y for phosphorylation; M and C for oxidation; and N and Q for deamidation. Complete elimination

Table 2. hERG Peptides and Their PRM Parameters

peptide	M.W.	transitions	charge	light M/Z	heavy M/Z	NCE[a]	LLOQ_1[b] (fmol)	LLOQ_2 (fmol)
ALVGPGSPPR	949.53	**precursor**	2	475.7745	480.7787	22	0.1	0.6
		precursor $[M+1]$	2	476.276	481.2802		0.4	0.1
		precursor $[M+2]$	2	476.7773	481.7815		0.6	n.a.
		b2	1	185.1285	185.1285		2	8
		b3	1	284.1969	284.1969		0	0
		b9	1	776.4301	776.4301		n.a.	n.a.
		y3	1	369.2245	379.2327		0	0
		y6	1	610.3307	620.339		0	0.1
		y7	1	667.3522	677.3605		0.08	0.4
		y7	2	334.1797	339.1839		0	0
		y6	2	305.669	310.6731		0	0
SAPGQLPSPR	1008.54	**precursor**	2	505.2749	510.279	32	1	2
		precursor $[M+1]$	2	505.7763	510.7805		1	2
		precursor $[M+2]$	2	506.2776	511.2818		4	n.a.
		b2	1	159.0764	159.0764		n.a.	n.a.
		y8	1	851.4734	861.4816		0	0
		y7	1	754.4206	764.4289		0	1
		y6	1	697.3991	707.4074		0	0.8
		y5	1	569.3406	579.3488		0	0.4
		y4	1	456.2565	466.2648		0	0
		y2	1	272.1717	282.18		0	0
		y8	2	426.2403	431.2445		n.a.	n.a.
AHSLNPDASGSSC[+57]SLAR	1728.78	**precursor**	2	865.3997	870.4039	27	1	0.8
		precursor $[M+1]$	2	865.9011	870.9053		2	2
		precursor $[M+2]$	2	866.402	871.4061		0.1	14
		b3	1	296.1353	296.1353		0	n.a.
		b4	1	409.2194	409.2194		n.a.	n.a.
		b5	1	523.2623	523.2623		0	0
		b7	1	735.342	735.342		n.a.	n.a.
		y13	1	1321.58	1331.588		0	0
		y12	1	1207.537	1217.545		0	0
		y10	1	995.4575	1005.466		0	0
		y9	1	924.4204	934.4286		0	0.6
SGLLNSTSDSDLVR	1462.73	**precursor**	2	732.3705	737.3746	22	1	2
		precursor $[M+1]$	2	732.8719	737.8761		3	2
		precursor $[M+2]$	2	733.3732	738.3774		4	n.a.
		b3	1	258.1448	258.1448		0	1
		b4	1	371.2289	371.2289		0	2
		y11	1	1206.596	1216.604		0.4	0.02
		y10	1	1093.512	1103.52		0.008	0.02
		y9	1	979.4691	989.4773		0.2	4
		y8	1	892.4371	902.4453		0.06	0.1
		y7	1	791.3894	801.3976		0	0.1
		y6	1	704.3573	714.3656		0	0.4

[a]NCE: normalized collision energy. [b]LLOQ: lower limit of quantitation for on-column peptide amount; and 1 and 2 for the two HML analyses, in which the second had 5-fold sample amount as of the first analysis.

of these amino acids during peptide selection is almost impossible. To identify suitable peptides as surrogates for hERG, we studied HEK-293T cells transiently transfected with the KCNH2 gene using shotgun proteomics and the DDA method, as described above. Table 1 summarizes the peptides that were frequently detected. Among them, four frequently detected peptides were selected (highlighted in red in Table 1) for customized synthesis as surrogates to quantify hERG, i.e., AHSLNPDASGSSCSLAR (AHS), ALVGPGSPPR (ALV), SAPGQLPSPR (SAP), and SGLLNSTSDSDLVR (SGL). Three (i.e., ALV, SAP, and AHS) of these peptides are adjacent to each other; therefore, their quantity can help determine

digestion efficiency. Their positions with respect to the lipid bilayer was visualized by Protter,[40] as shown in Figure 1.

The optimized NCE for each peptide is summarized in Table 2, and the corresponding fragmentation patterns are shown in Figure 2. Different from multiple reaction monitoring (MRM) approaches[26,39] in which the quantitation fragments need to be predetermined, the PRM approach carried out by Orbitrap records the entire MS2 spectra from the target peptides. Therefore, there was no need to select the target fragments for detection. The flexibility of choosing from a range of fragments ensures successful quantitation with less optimization. To provide enough choices, we evaluated the top 8 fragment ions from each peptide together with their corresponding precursor
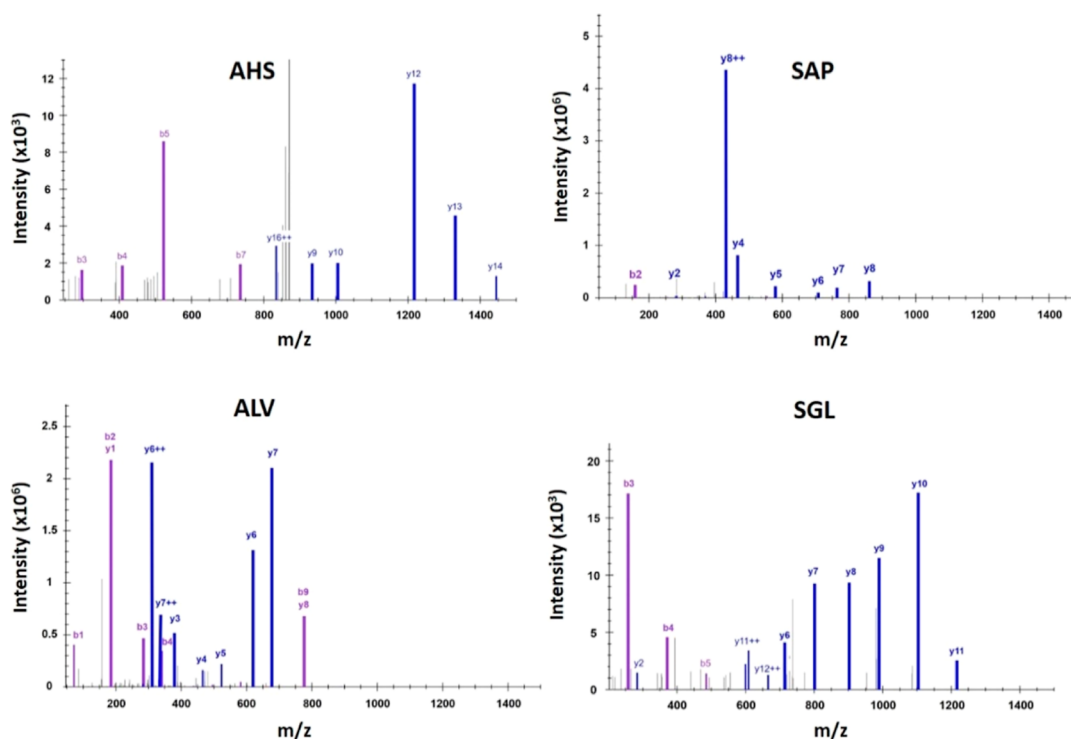
Figure 2. Fragmentation patterns of targeted hERG peptides. Purple denotes b ions originated from the N termini, and blue denotes y ions originated from the C termini.

ions during assay development. Table 2 summarizes all the evaluated transitions, including their accurate isotopic mass-to-charge ratios and the corresponding NCE. The transitions with LLOQ values were used for quantitation.

Evaluation of the Selected Transitions in the Authentic Matrix. Matrix effect is paramount to the assay performance, including the sensitivity, LLOQ, and accuracy.[31] The most appropriate evaluation of different candidate transitions requires the use of an authentic matrix. Unfortunately, it is technically challenging to obtain an authentic and complex biological matrix without the endogenous proteins in the sample. The complexity of the authentic matrix prevents the simple mixing of a few different proteins to represent the authentic complexity,[41] and the depletion of the target analyte from the original sample to obtain an authentic matrix is limited by depletion efficiency and selectivity. For example, in the present study of hERG expressed in HEK293T cells, the closest alternative to the authentic matrix was HEK293T cells transfected with the empty plasmid. However, the expression of foreign proteins can perturb the host cell proteome, and such perturbations are often protein- and transfection-specific and difficult to mimic. Therefore, the most accurate evaluation of the performance of different transitions is in-sample calibration, in which a calibration curve is built within the sample matrix where the endogenous analytes reside.

Two targeted MS methods can achieve in-sample calibration. One is the popular SA approach, in which a heavy synthetic isotopologue of the endogenous analyte is used as the internal standard spiked into the sample at a constant concentration, and a light synthetic isotopologue identical to the endogenous counterpart is used as the calibrator, which is spiked into the sample at various concentrations. The intercept of the calibration curve generated by the SA method was used to calculate the endogenous protein concentration. However, such

methods require the use of two isotopologues for the internal standards and for the calibrators. We developed a single-isotopologue in-sample calibration method using HML mathematical treatment to obtain the endogenous analyte quantity.[31] This method used heavy synthetic isotopologues as the calibrators and sample endogenous peptides as the internal standards. As a result, the HML approach swaps the calibrators and internal standards in the SA method and eliminates the need for the second isotopologue as the internal standard.

Here, we employed both SA and HML to evaluate the assay performance. The raw MS files acquired via the PRM approach by Q Exactive HF were analyzed by Skyline software.[35] Due to the complexity of the matrix, skyline-extracted chromatographs contained multiple signal peaks. We used the following criteria to manually verify all the target signals: (1) an overlap of peak retention times between the light and heavy peptides; (2) for the same peptide precursor, an overlap of peak retention times among all the transitions; (3) a matching retention time between the results of Skyline and Discoverer on the same raw file, in which the corresponding peptide sequences were identified; and (4) a consistent trend of variation between the concentrations of the spike-in peptides and the integrated peak areas. Examples of extracted signal peaks for both heavy and light peptides in Skyline are shown in Figure 3A−C.

An example of a combined calibration curve for 3 technical replicates of every peptide is shown in Figure 3D. A total of 165 calibration curves were obtained, including their corresponding slopes, intercepts, and R^2 (coefficient of determination) values. To eliminate the low-quality transitions potentially from the matrix effect, we used the criterion of R^2 above 0.96 to filter all the calibration curves. Then, we obtained the LLOQ for the results from the HML method,[31] in which conditions with zero concentrations of the heavy reference peptides were available. The LLOQ cannot be assessed from the SA method owing to the
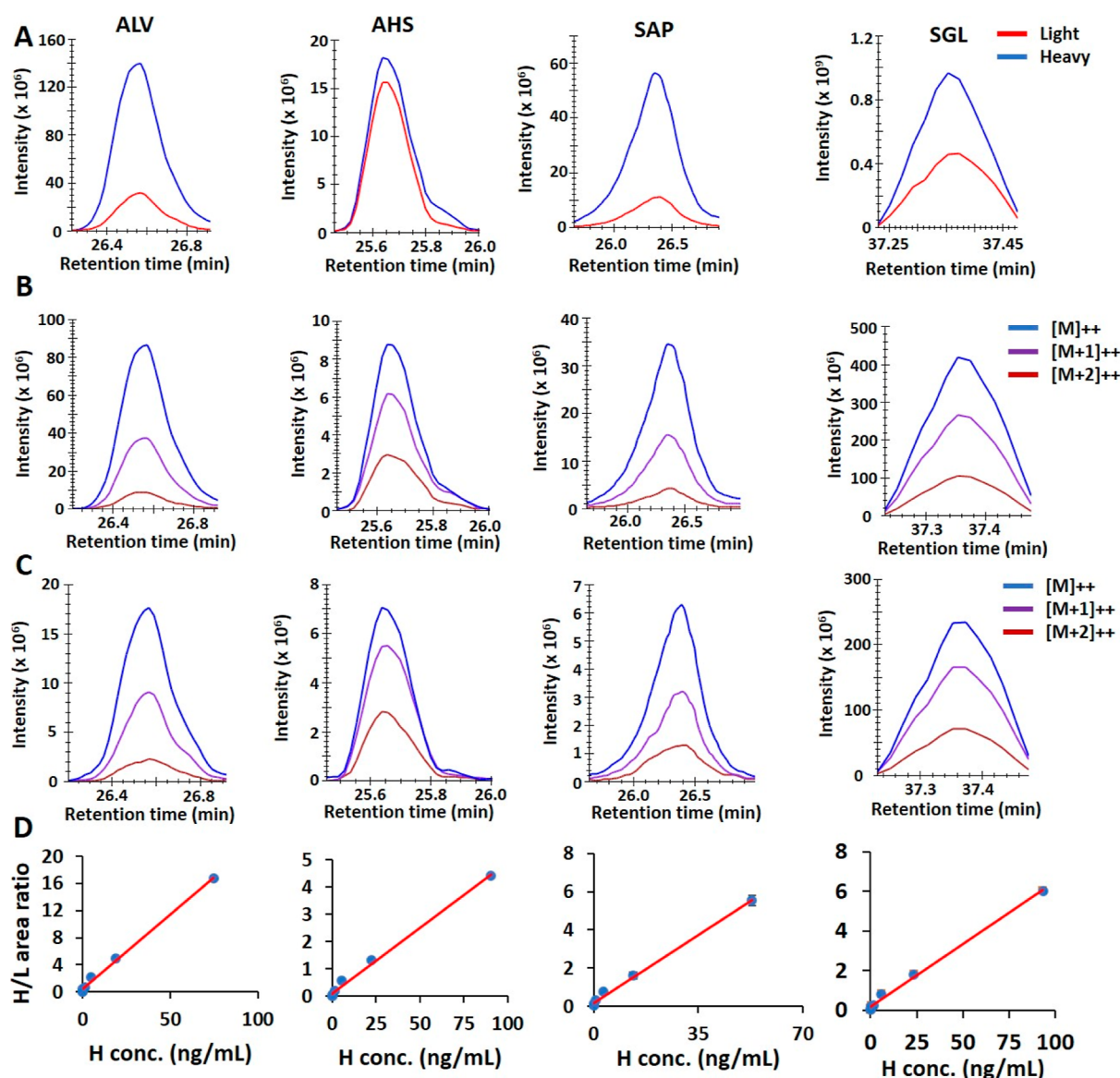
Figure 3. PRM results of the selected peptides. (A) Examples of the total extracted chromatograms for heavy and light target peptides. (B) Corresponding extracted chromatograms of heavy precursors. (C) Corresponding extracted chromatograms of light precursors. (D) Corresponding calibration curves established for the area ratio between the precursor M of heavy and light peptides as a function of 8 concentrations of heavy peptides (the error bar is the standard deviation of three replications).
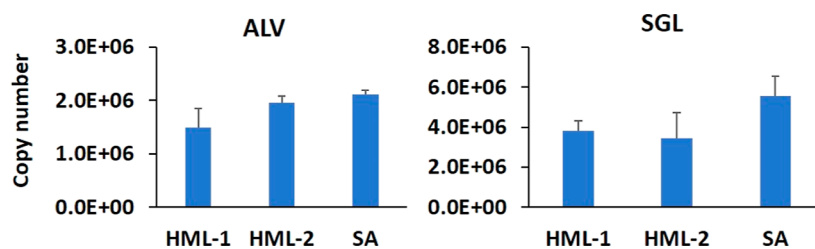

Figure 4. Comparison between two in-sample calibration approaches (heavy-match-light, HML, approach, and the standard addition, SA, approach) for ALV and SGL peptides from hERG. The error bar is the standard deviation of three replicates. There was no statistically significant difference between these studies ($p > 0.05$).

lack of such conditions. The HML method was repeated once to evaluate assay reproducibility. In the second HML analysis, the sample quantity was increased 5 times, while the concentrations of the heavy reference peptides were kept the same to better

assess the matrix effect. The on-column LLOQs in fmol for a 2 μL injection volume are summarized in Table 2.

In general, fragment transitions had lower LLOQ values than their corresponding precursors, suggesting that fragments were less impacted by background noise. In addition, when

comparing the two repeated HML analyses, more than half of the LLOQs showed increased values in the one with more matrix, one-third had no effect, and only 10% showed the opposite changes. This observation indicated that LLOQ values are sensitive to matrix effects. Finally, all the selected peptides had comparable LLOQs, and ALV, SAP, and AHS in particular had overall LLOQs less than 1 fmol, as determined by averaging all the LLOQs of their transitions.

Quantification of the Endogenous hERG in the Sample. To evaluate the results, we first compared the quantities obtained by the HML and SA methods. We selected two peptides (ALV and SGL) for this comparison. Figure 4 shows the comparison results, in which the HML method had two repeats. For both peptides, the three sets of measurements regardless of methods obtained similar copy numbers with no statistically significant changes (t-test). These results confirmed the robustness of the assay. Compared to the SA method, HML is simpler in terms of experimental requirements, in which only heavy reference peptides are needed, whereas the SA method requires both heavy reference peptides as internal standards and light reference peptides matching endogenous peptides as calibrators. The internal standards do exist in the HML method, and they are endogenous peptides present in the sample. In addition, the HML method can offer LLOQ values of the assay. The reason is that the HML method uses heavy isotopologues as calibrators, and these peptides are absent from the original sample; therefore, their background can be accurately measured.

Second, we compared the copy numbers of hERG obtained from all four peptides by the HML method. Figure 5A summarizes the initial results. To our satisfactory, all selected peptides except ALV had similar copy numbers because all these peptides were derived from the same protein. We further

investigated the cause of difference in ALV copy number. Several factors might contribute to this difference, and the most frequent concern was digestion efficiency. ALV is located at the N-terminus of the peptide trio that we selected to evaluate the digestion efficiency. The lower quantity exclusively from ALV suggested that incomplete digestion would be resolved from the N-terminus tryptic end of ALV as opposed to the C-terminus tryptic end. Interestingly, an exceptionally long tryptic peptide (50 amino acids in length) resides immediately before the ALV peptide, and it was successfully detected by the DDA method in the same sample, as shown in Table 1 (highlighted in green). The spectra counting method used on DDA results can roughly estimate the quantity of peptides.[42] We and others have used it to quantify protein quantity in a number of systems.[43,44] Based on the spectra counts, i.e., PSM values, the peptide quantity summarized in Table 1 correlated with the peptide quantity (Figure 5) measured by PRM. The leading peptide (abbreviated as SGG) prior to ALV in Table 1 was identified in two forms, one with an additional Arg. The sum of the PSMs of these two SGG forms was similar to that of SAP, which is trailing ALV. Both SGG and SAP had greater quantities than ALV itself. No Arg-attached ALV was detected. These observations suggested that digestion might not be the culprit.

We then considered post-translational modifications. UniProt indicates that ALV has a potential phosphorylation site at S239. To confirm this hypothesis, we researched our DDA results by adding S or T phosphorylation as an additional dynamic modification. This allowed us to identify the phosphorylated ALV together with two other phosphopeptides, as shown in Table 1. Adding the PSM value of the newly detected phospho-ALV made the total spectra counts of ALV similar to those of SGG and SAP. Encouraged by this discovery, we used PRM to quantify the phosphorylated ALV from the precursor transitions. When the quantity of phosphorylated ALV was added to the quantity of nonphosphorylated ALV, the copy number obtained from ALV was similar to the rest, as shown in Figure 5B. Phosphorylation has been detected in hERG, and both protein kinase A[45] and protein kinase C[46] are known to modify this protein. However, S239 phosphorylation in hERG was not detected previously by site-directed mutagenesis but rather by phosphoproteomic analysis of a cancer cell line.[47] Our targeted MS analysis further confirmed this modification in the heterologous expression system.

The final copy number of hERG inferred from the four selected peptides was 3.6 ± 0.5 million/cell by HML, and no significant difference was observed among the four peptides based on one-way ANOVA. These results also agreed with the copy number measured by the SA method for the two peptides, i.e., 5 ± 1 million/cell. The precision of the HML method was slightly greater, as determined by a 15% coefficient of variation (CV), than was that of the SA method, which was 20%, mainly because we used more peptides in the HML analysis. Considering that the Kv11.1 channel is a tetramer, the total copy number of the Kv11.1 channel in the analyzed HEK293T-hERG can reach approximately 1 million/cell.

Western Blot Analysis. We used Western blotting to confirm the expression of hERG. Figure 6 shows the results. In the transfected HEK293T-hERG sample, a thick hERG band above 130 kDa and below 180 kDa was observed. This signal was absent from the control HEK239T sample. Carrying two N-glycosylation sites, matured hERG are known to exhibit two bands ranging from 132 to 155 kd[6,14,15] on Western blot, and various glycoforms can result in glycoproteins that appear as a
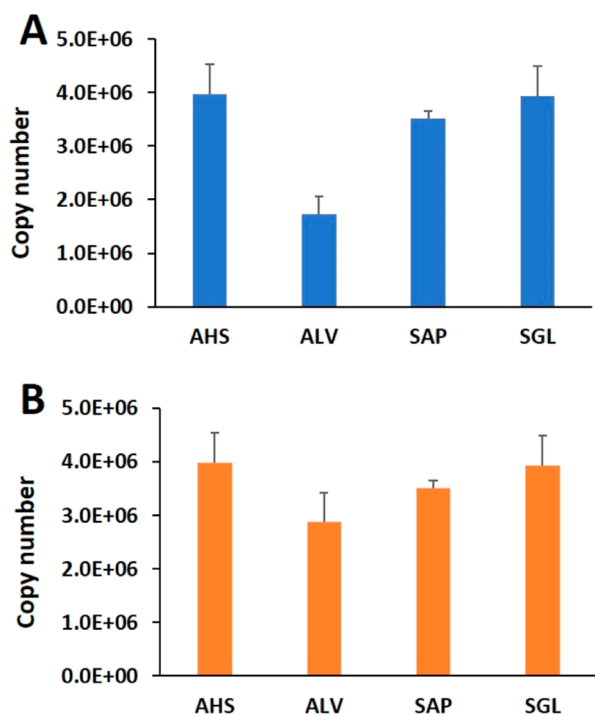

Figure 5. Copy number of hERG was quantified by the surrogate peptides using the HML method. The error bar is the standard deviation between two HML analyses. (A) Results before considering ALV phosphorylation. (B) Results after adjusting ALV phosphorylation.
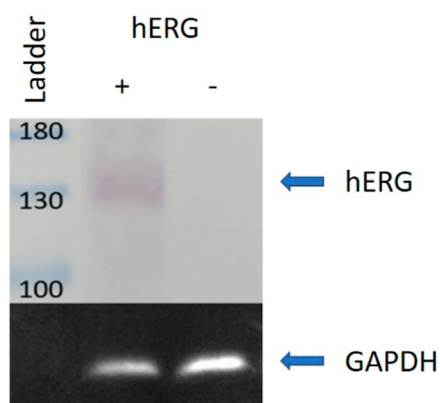
Figure 6. Western image of the HEK293T cell lysate against hERG and GAPDH.

smear band in SDS−PAGE. Our results were consistent with those of previous reports. The GAPDH loading control signal was less intense in the transfected sample than in the control sample even though an equal amount of protein was loaded, suggesting potential normalization bias in GAPDH.

To verify the quantity of Kv11.1 obtained by our PRM assay, we examined published results from single-channel and whole-cell patch clamp recordings. Kiehn et al.[48] and others[49] reported that the conductance of a single Kv11.1 channel at a physiological KCl concentration and 0 mV was approximately 2 pS. The mean channel opening probability can be calculated as ~0.1 based on the 3.2 ms opening time and 1.0 and 26 ms closing times reported by Kiehn et al.[48] It is reasonable to assume a 2 nA tail current from a whole-cell recording under similar physiological conditions for a HEK293-hERG-transfected cell[10,19,21,49−51] and a 0.2 nS macroconductance. Using $G = g \times N \times Po$, where G is the macroconductance, g is the single-channel conductance, N is the number of channels in the specified area, and Po is the probability of channel opening, we can approximate a channel number/cell of $\sim 1 \times 10^6$. This estimated value is in the same order of our measurement. Transiently transfected cells can carry a large variation in the tail current ranging from 1 to 10 nA,[52] and our quantitation helps to link the measured whole-cell current to copy numbers of the channel.

CONCLUSIONS

In this study, four peptides identified from HEK-293T cells transfected with the KCNH2 gene were selected as surrogates for absolute quantification of hERG and Kv11.1 copy numbers. The samples were analyzed via PRM on a Q Exactive HF instrument with an Orbitrap mass analyzer. In total, 11 transitions (3 precursor transitions and 8 fragment transitions) for each peptide were evaluated by building 8-concentration calibration curves using two methods, i.e., SA and HML, for in-sample calibration. Moreover, HML was carried out twice during different weeks with different sample concentrations. After filtering the calibration curves with a linearity cutoff of $R^2 > 0.96$ and further removing residual outliers by the Q test, we obtained 3.6 million copies/cell of hERG protein with a CV of 15%.

The assay exhibited high sensitivity, with on-column LLOQs ranging from attomole to lower femtomole, as shown in Table 2. Compared to traditional quantitative immunoassays, whose LLOQs are usually around 0.1−20 pmol,[53−58] targeted MS

approaches do not require antibodies and are more sensitive and accurate. Compared with SRM and MRM, PRM offered us the flexibility to monitor any number of transitions. Table 2 shows that variations in LLOQs exist among different transitions. Furthermore, the LLOQs also showed variations when the matrix was changed according to the two HML analyses. Therefore, the flexibility offered by PRM in choosing suitable transitions is critical to ensure efficient quantitation with minimum optimization time. The expression of hERG was confirmed by Western blot, and the measured quantity agreed with reports from single-cell and whole-cell electrophysiological measurements.

The ability to quantify hERG protein copies will help advance functional studies of hERG in health and disease. Such absolute quantitation also enables comparisons between hERG and other ion channel proteins that were traditionally examined for fold changes relative to their respective controls and cannot be compared directly. For example, we had quantified the copy number of Nav1.5, expressed in Chinese hamster ovary cells, on the order of tens of thousands of copies/cell.[34] The copy number differences observed in hERG and Nav1.5 from the two expression systems were comparable and collectively showed variations among the different expression systems. Similar differences in the expression of these ion channels have also been reported in patch-clamp functional studies of single cells.[52] Our bulk analysis using MS can effectively describe global quantities, whereas single-cell studies require a large number of analyses to reflect the bulk condition.

AUTHOR INFORMATION

Corresponding Author

Bingyun Sun − *Department of Chemistry, Simon Fraser University, Burnaby, British Columbia V5A1S6, Canada;* orcid.org/0000-0002-4132-6942; Email: bingyun_sun@sfu.ca

Authors

Ge Chang − *Department of Chemistry, Simon Fraser University, Burnaby, British Columbia V5A1S6, Canada*
Fabusuyi A. Aroge − *School of Mechatronic Systems Engineering, Simon Fraser University, Surrey, British Columbia V3T0A3, Canada*
Ravichandra Venkateshappa − *Department of Biomedical Physiology and Kinesiology, Simon Fraser University, Burnaby, British Columbia V5A1S6, Canada*
Tom W. Claydon − *Department of Biomedical Physiology and Kinesiology, Simon Fraser University, Burnaby, British Columbia V5A1S6, Canada*

Complete contact information is available at:
https://pubs.acs.org/10.1021/acsomega.4c04541

Notes

The authors declare no competing financial interest.

■ REFERENCES

(1) Foo, B.; Williamson, B.; Young, J. C.; Lukacs, G.; Shrier, A. hERG quality control and the long QT syndrome. *J. Physiol.* **2016**, *594* (9), 2469−2481.

(2) Gutman, G. A.; Chandy, K. G.; Adelman, J. P.; Aiyar, J.; Bayliss, D. A.; Clapham, D. E.; Covarriubias, M.; Desir, G. V.; Furuichi, K.; Ganetzky, B.; et al. International Union of Pharmacology. XLI. Compendium of voltage-gated ion channels: potassium channels. *Pharmacol. Rev.* **2003**, *55* (4), 583−586.

(3) Vandenberg, J. I.; Perry, M. D.; Perrin, M. J.; Mann, S. A.; Ke, Y.; Hill, A. P. hERG K(+) channels: structure, function, and clinical significance. *Physiol. Rev.* **2012**, *92* (3), 1393−1478.

(4) Smith, P. L.; Baukrowitz, T.; Yellen, G. The inward rectification mechanism of the HERG cardiac potassium channel. *Nature* **1996**, *379* (6568), 833−836.

(5) Curran, M. E.; Splawski, I.; Timothy, K. W.; Vincen, G.; Green, E. D.; Keating, M. T. A molecular basis for cardiac arrhythmia: HERG mutations cause long QT syndrome. *Cell* **1995**, *80* (5), 795−803.

(6) Sanguinetti, M. C.; Jiang, C.; Curran, M. E.; Keating, M. T. A mechanistic link between an inherited and an acquird cardiac arrthytmia: HERG encodes the IKr potassium channel. *Cell* **1995**, *81* (2), 299−307.

(7) Butler, A.; Zhang, Y.; Stuart, A. G.; Dempsey, C. E.; Hancox, J. C. Functional and pharmacological characterization of an S5 domain hERG mutation associated with short QT syndrome. *Heliyon* **2019**, *5* (4), No. e01429.

(8) Campuzano, O.; Fernandez-Falgueras, A.; Lemus, X.; Sarquella-Brugada, G.; Cesar, S.; Coll, M.; Mates, J.; Arbelo, E.; Jordà, P.; Perez-Serra, A.; et al. Short QT Syndrome: A Comprehensive Genetic Interpretation and Clinical Translation of Rare Variants. *J. Clin. Med.* **2019**, *8* (7), 1035.

(9) Haverkamp, W.; et al. The potential for QT prolongation and proarrhythmia by non-antiarrhythmic drugs: clinical and regulatory implications. Report on a policy conference of the European Society of Cardiology. *Eur. Heart J.* **2000**, *21* (15), 1216−1231.

(10) Lamothe, S. M.; Song, W.; Guo, J.; Li, W.; Yang, T.; Baranchuk, A.; Graham, C. H.; Zhang, S. Hypoxia reduces mature hERG channels through calpain up-regulation. *FASEB J.* **2017**, *31* (11), 5068−5077.

(11) Lastraioli, E.; Guasti, L.; Crociani, O.; Polvani, S.; Hofmann, G.; Witchel, H.; Bencini, L.; Calistri, M.; Messerini, L.; Scatizzi, M.; et al. herg1 gene and HERG1 protein are overexpressed in colorectal cancers and regulate cell invasion of tumor cells. *Cancer Res.* **2004**, *64* (2), 606−611.

(12) Cherubini, A.; Taddei, G. L.; Crociani, O.; Paglierani, M.; Buccoliero, A. M.; Fontana, L.; Noci, I.; Borri, P.; Borrani, E.; Giachi, M.; et al. HERG potassium channels are more frequently expressed in human endometrial cancer as compared to non-cancerous endometrium. *Br. J. Cancer* **2000**, *83* (12), 1722−1729.

(13) He, S.; Moutaoufik, M. T.; Islam, S.; Persad, A.; Wu, A.; Aly, K. A.; Fonge, H.; Babu, M.; Cayabyab, F. S. HERG channel and cancer: A mechanistic review of carcinogenic processes and therapeutic potential. *Biochim. Biophys. Acta, Rev. Cancer* **2020**, *1873* (2), 188355.

(14) Pillozzi, S.; Brizzi, M.; Balzi, M.; Crociani, O.; Cherubini, A.; Guasti, L.; Bartolozzi, B.; Becchetti, A.; Wanke, E.; Bernabei, P.; et al. HERG potassium channels are constitutively expressed in primary human acute myeloid leukemias and regulate cell proliferation of normal and leukemic hemopoietic progenitors. *Leukemia* **2002**, *16* (9), 1791−1798.

(15) Jones, D. K.; Liu, F.; Vaidyanathan, R.; Eckhardt, L. L.; Trudeau, M. C.; Robertson, G. A. hERG 1b is critical for human cardiac repolarization. *Proc. Natl. Acad. Sci. U.S.A.* **2014**, *111* (50), 18073−18077.

(16) Ballouz, S.; Mangala, M. M.; Perry, M. D.; Heitmann, S.; Gillis, J. A.; Hill, A. P.; Vandenberg, J. I. Co-expression of calcium and hERG potassium channels reduces the incidence of proarrhythmic events. *Cardiovasc. Res.* **2021**, *117* (10), 2216−2227.

(17) Koussounadis, A.; Langdon, S. P.; Um, I. H.; Harrison, D. J.; Smith, V. A. Relationship between differentially expressed mRNA and mRNA-protein correlations in a xenograft model system. *Sci. Rep.* **2015**, *5* (1), 10775.

(18) de Sousa Abreu, R.; Penalva, L. O.; Marcotte, E. M.; Vogel, C. Global signatures of protein and mRNA expression levels. *Mol. Biosyst.* **2009**, *5* (12), 1512−1526.

(19) Feng, P. F.; Zhang, B.; Zhao, L.; Fang, Q.; Liu, Y.; Wang, J. N.; Xu, X. Q.; Xue, H.; Li, Y.; Yan, C. C.; et al. Intracellular Mechanism of Rosuvastatin-Induced Decrease in Mature hERG Protein Expression on Membrane. *Mol. Pharm.* **2019**, *16* (4), 1477−1488.

(20) Shi, Y. Q.; Yan, M.; Liu, L. R.; Zhang, X.; Wang, X.; Geng, H. Z.; Zhao, X.; Li, B. X. High Glucose Represses hERG K+ Channel Expression through Trafficking Inhibition. *Cell. Physiol. Biochem.* **2015**, *37* (1), 284−296.

(21) Zhou, Z.; Gong, Q.; Ye, B.; Fan, Z.; Makielski, J. C.; Robertson, G. A.; January, C. T. Properties of HERG channels stably expressed in HEK 293 cells studied at physiological temperature. *Biophys. J.* **1998**, *74* (1), 230−241.

(22) Ho, K. H.; Patrizi, A. Assessment of common housekeeping genes as reference for gene expression studies using RT-qPCR in mouse choroid plexus. *Sci. Rep.* **2021**, *11* (1), 3278.

(23) Townsend, M. H.; Felsted, A. M.; Ence, Z. E.; Piccolo, S. R.; Robison, R. A.; O'Neill, K. L. Falling from grace: HPRT is not suitable as an endogenous control for cancer-related studies. *Mol. Cell. Oncol.* **2019**, *6* (2), 1575691.

(24) Ruiz-Villalba, A.; Mattiotti, A.; Gunst, Q. D.; Cano-Ballesteros, S.; van den Hoff, M. J. B.; Ruijter, J. M. Reference genes for gene expression studies in the mouse heart. *Sci. Rep.* **2017**, *7* (1), 24.

(25) Karnik, R.; Ludlow, M. J.; Abuarab, N.; Smith, A. J.; Hardy, M. E. L.; Elliott, D. J. S.; Sivaprasadarao, A. Endocytosis of HERG is clathrin-independent and involves arf6. *PLoS One* **2013**, *8* (12), No. e85630.

(26) Vidova, V.; Spacil, Z. A review on mass spectrometry-based quantitative proteomics: Targeted and data independent acquisition. *Anal. Chim. Acta* **2017**, *964*, 7−23.

(27) Barr, J. R.; Maggio, V. L.; Patterson, D. G.; Cooper, G. R.; Henderson, L. O.; Turner, W. E.; Smith, S. J.; Hannon, W. H.; Needham, L. L.; Sampson, E. J. Isotope dilution−mass spectrometric quantification of specific proteins: model application with apolipoprotein A-I. *Clin. Chem.* **1996**, *42* (10), 1676−1682.

(28) Gerber, S. A.; Rush, J.; Stemman, O.; Kirschner, M. W.; Gygi, S. P. Absolute quantification of proteins and phosphoproteins from cell lysates by tandem MS. *Proc. Natl. Acad. Sci. U.S.A.* **2003**, *100* (12), 6940−6945.

(29) Barnidge, D. R.; Dratz, E. A.; Martin, T.; Bonilla, L. E.; Moran, L. B.; Lindall, A. Absolute quantification of the G protein-coupled receptor rhodopsin by LC/MS/MS using proteolysis product peptides and synthetic peptide standards. *Anal. Chem.* **2003**, *75* (3), 445−451.

(30) Kuzyk, M. A.; Smith, D.; Yang, J.; Cross, T. J.; Jackson, A. M.; Hardie, D. B.; Anderson, N. L.; Borchers, C. H. Multiple reaction monitoring-based, multiplexed, absolute quantitation of 45 proteins in human plasma. *Mol. Cell. Proteomics* **2009**, *8* (8), 1860−1877.

(31) Torkamannejad, S.; Chang, G.; Aroge, F. A.; Sun, B. Single Isotopologue for In-Sample Calibration and Absolute Quantitation by LC-MS/MS. *J. Proteome Res.* **2024**, *23* (4), 1351−1359.

(32) Ranade, A. V.; Mukhtarov, R.; An Liu, K. J.; Behrner, M. A.; Sun, B. Characterization of sample loss caused by competitive adsorption of proteins in vials using sodium dodecyl sulfate−polyacrylamide gel electrophoresis. *Langmuir* **2019**, *35* (12), 4224−4232.

(33) Sun, B.; Kovatch, J. R.; Badiong, A.; Merbouh, N. Optimization and modeling of quadrupole orbitrap parameters for sensitive analysis toward single-cell proteomics. *J. Proteome Res.* **2017**, *16* (10), 3711−3721.

(34) Adams, S. L.; Chang, G.; Fouda, M.; Kumar, S.; Sun, B. Absolute Quantification of Nav1.5 Expression by Targeted Mass Spectrometry. *Int. J. Mol. Sci.* **2022**, *23* (8), 4177.

(35) Pino, L. K.; Searle, B. C.; Bollinger, J. G.; Nunn, B.; MacLean, B.; MacCoss, M. J. The Skyline ecosystem: Informatics for quantitative mass spectrometry proteomics. *Mass Spectrom. Rev.* **2020**, *39* (3), 229−244.

(36) Currie, L. A. Limits for qualitative detection and quantitative determination. Application to radiochemistry. *Anal. Chem.* **1968**, *40* (3), 586−593.

(37) Dean, R. B.; Dixon, W. J. Simplified statistics for small numbers of observations. *Anal. Chem.* **1951**, *23* (4), 636−638.

(38) Rorabacher, D. B. Statistical treatment for rejection of deviant values: critical values of Dixon's Q parameter and related subrange ratios at the 95% confidence level. *Anal. Chem.* **1991**, *63* (2), 139−146.

(39) Peterson, A. C.; Russell, J. D.; Bailey, D. J.; Westphall, M. S.; Coon, J. J. Parallel reaction monitoring for high resolution and high mass accuracy quantitative, targeted proteomics. *Mol. Cell. Proteomics* **2012**, *11* (11), 1475−1488.

(40) Omasits, U.; Ahrens, C. H.; Müller, S.; Wollscheid, B. Protter: interactive protein feature visualization and integration with experimental proteomic data. *Bioinformatics* **2014**, *30* (6), 884−886.

(41) Jones, B. R.; Schultz, G. A.; Eckstein, J. A.; Ackermann, B. L. Surrogate matrix and surrogate analyte approaches for definitive quantitation of endogenous biomolecules. *Bioanalysis* **2012**, *4* (19), 2343−2356.

(42) Liu, H.; Sadygov, R. G.; Yates, J. R. A model for random sampling and estimation of relative protein abundance in shotgun proteomics. *Anal. Chem.* **2004**, *76* (14), 4193−4201.

(43) Paoletti, A. C.; Parmely, T. J.; Tomomori-Sato, C.; Sato, S.; Zhu, D.; Conaway, R. C.; Conaway, J. W.; Florens, L.; Washburn, M. P. Quantitative proteomic analysis of distinct mammalian Mediator complexes using normalized spectral abundance factors. *Proc. Natl. Acad. Sci. U.S.A.* **2006**, *103* (50), 18928−18933.

(44) Sun, B.; Ma, L.; Yan, X.; Lee, D.; Alexander, V.; Hohmann, L. J.; Lorang, C.; Chandrasena, L.; Tian, Q.; Hood, L. N-Glycoproteome of E14.Tg2a mouse embryonic stem cells. *PLoS One* **2013**, *8* (2), No. e55722.

(45) Thomas, D.; Zhang, W.; Karle, C. A.; Kathöfer, S.; Schöls, W.; Kübler, W.; Kiehn, J. Deletion of protein kinase A phosphorylation sites in the HERG potassium channel inhibits activation shift by protein kinase A. *J. Biol. Chem.* **1999**, *274* (39), 27457−27462.

(46) Thomas, D.; et al. Regulation of HERG potassium channel activation by protein kinase C independent of direct phosphorylation of the channel protein. *Cardiovasc. Res.* **2003**, *59* (1), 14−26.

(47) Zhou, H.; Di Palma, S.; Preisinger, C.; Peng, M.; Polat, A. N.; Heck, A. J. R.; Mohammed, S. Toward a comprehensive characterization of a human cancer cell phosphoproteome. *J. Proteome Res.* **2013**, *12* (1), 260−271.

(48) Kiehn, J.; Lacerda, A. E.; Wible, B.; Brown, A. M. Molecular physiology and pharmacology of HERG. Single-channel currents and block by dofetilide. *Circulation* **1996**, *94* (10), 2572−2579.

(49) Wilson, S. L.; Dempsey, C. E.; Hancox, J. C.; Marrion, N. V. Identification of a proton sensor that regulates conductance and open time of single hERG channels. *Sci. Rep.* **2019**, *9* (1), 19825.

(50) Paulussen, A.; Raes, A.; Matthijs, G.; Snyders, D. J.; Cohen, N.; Aerssens, J. A novel mutation (T65P) in the PAS domain of the human potassium channel HERG results in the long QT syndrome by trafficking deficiency. *J. Biol. Chem.* **2002**, *277* (50), 48610−48616.

(51) Wang, W.; MacKinnon, R. Cryo-EM Structure of the Open Human Ether-à-go-go-Related K+ Channel hERG. *Cell* **2017**, *169* (3), 422−430.e10.

(52) Trapani, J. G.; Korn, S. J. Control of ion channel expression for patch clamp recordings using an inducible expression system in mammalian cell lines. *BMC Neurosci.* **2003**, *4*, 15.

(53) Biffiger, K.; Zwald, D.; Kaufmann, L.; Briner, A.; Nayki, I.; Pürro, M.; Böttcher, S.; Struckmeyer, T.; Schaller, O.; Meyer, R.; et al. Validation of a luminescence immunoassay for the detection of PrPSc in brain homogenate. *J. Virol. Methods* **2002**, *101* (1−2), 79−84.

(54) Deslys, J. P.; Comoy, E.; Hawkins, S.; Simon, S.; Schimmel, H.; Wells, G.; Grassi, J.; Moynagh, J. Screening slaughtered cattle for BSE. *Nature* **2001**, *409* (6819), 476−478.

(55) Grassi, J.; Simon, S.; Crminon, C.; Frobert, Y.; Comoy, E.; Trapmann, S.; Schimmel, H.; Hawkins, S. A. C.; Wells, G. H.; Moynagh, J.; et al. Rapid test for the preclinical postmortem diagnosis of BSE in central nervous system tissue. *Vet. Rec.* **2001**, *149* (19), 577−582.

(56) Lee, D. C.; Stenland, C. J.; Hartwell, R. C.; Ford, E. K.; Cai, K.; Miller, J. L.; Gilligan, K. J.; Rubenstein, R.; Fournel, M.; Petteway, S. R. Monitoring plasma processing steps with a sensitive Western blot assay for the detection of the prion protein. *J. Virol. Methods* **2000**, *84* (1), 77−89.

(57) Wadsworth, J.; Joiner, S.; Hill, A.; Campbell, T.; Desbruslais, M.; Luthert, P.; Collinge, J. Tissue distribution of protease resistant prion protein in variant Creutzfeldt-Jakob disease using a highly sensitive immunoblotting assay. *Lancet* **2001**, *358* (9277), 171−180.

(58) Safar, J. G.; Scott, M.; Monaghan, J.; Deering, C.; Didorenko, S.; Vergara, J.; Ball, H.; Legname, G.; Leclerc, E.; Solforosi, L.; et al. Measuring prions causing bovine spongiform encephalopathy or chronic wasting disease by immunoassays and transgenic mice. *Nat. Biotechnol.* **2002**, *20* (11), 1147−1150.